20

Ultra-fast Microwave Heating for Large Bandgap Semiconductor Processing

Mulpuri V. Rao
Department of Electrical and Computer Engineering
George Mason University, Fairfax, Virginia 22030,
U.S.A.

1. Introduction

The concept of using microwaves for fast semiconductor processing is known for the last three decades (Spinter et al., 1981; Scovell, 1984; Amada, 1987; Fukano et al., 1985; Zhang et al., 1994; Thompson et al., 2007). Conventional heating methods are slow because in these methods the heat is applied to the surface of the object to be heated, which needs to be transferred from the surface to the interior of the object by thermal conduction, requiring time for heating the whole object. In addition, in conventional heating methods we not only heat the object, but also the surrounding ambient, which slows down both heating and cooling rates. In contrast, microwave heating is fast because microwaves can permeate into objects heating both interior and exterior simultaneously. In addition, the ambient surrounding the object is not heated resulting in ultra-fast heating and cooling rates (Y. Tian & M.Y. Tian, 2009). It is this feature, which makes microwave heating attractive in semiconductor processing. This chapter focuses on the use of microwaves for large bandgap semiconductor material and device processing. More specifically, heating of semiconductors in a microwave cavity resonator and coupling of microwaves to a semiconductor using a microwave head are discussed. There are many applications of using microwave energy for ultra-fast thermal processing of semiconductors, such as impurity diffusion, annealing of ion-implantation generated lattice damage, ohmic contact alloying, nanowire growth etc. However, the primary focus of this chapter is on using microwave heating for annealing lattice damage in ion-implanted SiC and GaN and for growing SiC nanowires. Though microwave annealing can be used for processing any semiconductors, it is much more attractive in case of SiC, where ultra-fast heating (>1000 ^{o}C/s) to temperatures as high as 2100 ^{o}C is needed for achieving desirable electrical characteristics in ion-implantation doped material. Devices made of hexagonal polytypes of SiC and GaN are highly attractive for high-power, high-frequency and high-temperature electronic and also for optoelectronic applications.

2. Mechanisms of microwave heating

Interaction between electromagnetic field in the microwaves and the target material results in heating of the material. Mechanism and degree of interaction depends on type of the material. Materials with low complex dielectric constant are poor absorbers of microwave

energy and are not suitable for microwave heating, whereas materials with high complex dielectric constant (such as SiC) are excellent absorbers of microwave energy and hence are strong candidates for microwave heating. In case of conductors such as metals, microwaves are reflected with absorption taking place only within a skin depth of the metal (which is in the range of a fraction of a micrometer to few micro-meters, depending on the frequency of the microwaves) inducing eddy current and consequently heat therein. Hence, metals are not good for microwave heating in general, unless the thickness of the metal is less than or in the same range as its skin depth. Since, the thickness of metal layers used for contacts in semiconductor device fabrication are in the same order as the skin depth, microwave heating is suitable for contact alloying. Though semiconductors such as Si and GaN are not strong absorbers of microwave energy, the highly doped conductive regions at the surface of the substrates of these materials absorb microwaves reasonably well causing selective heating of the doped regions. Similarly, in case of semiconductor hetero-structures comprising layers of strong and poor absorbers of microwaves, microwave heating can be targeted to specific layers in the hetero-structures (Y. Tian & M.Y. Tian, 2009).

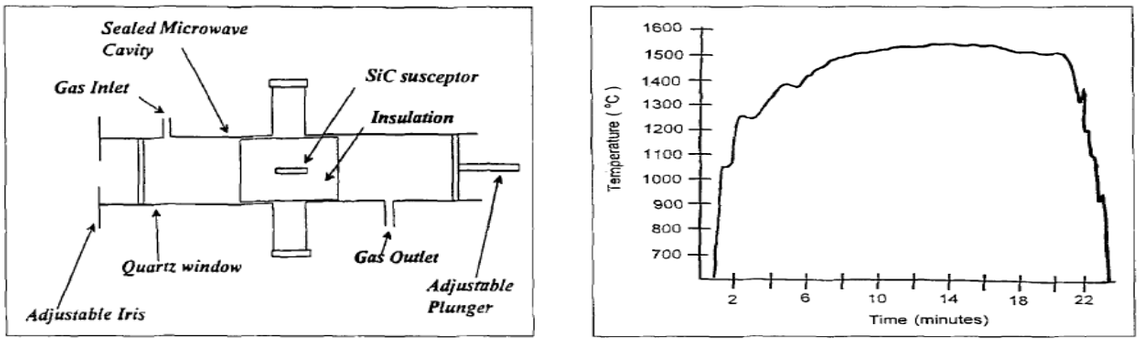

(a) (b)

Fig. 1. Schematics of (a) microwave cavity annealing system, and (b) Typical temperature/time cycle for 1500 ^{o}C/10min microwave cavity annealing on implanted SiC.

The heating rate of microwave thermal process depends on the intensity of microwave electromagnetic (EM) field and the EM energy coupled to the material to be heated. Obviously a high intensity EM field is required for high heating rate. The EM energy can be coupled to the material in three different ways. In capacitive coupling, the energy is coupled to the material via electric (E) field and in inductive coupling, the energy is coupled to the material via magnetic (H) field; where as in cavity coupling the energy is coupled to the material via a combination of E and H fields. Cavity coupling is the most widely used method among microwave heating processes. In this method, the heating furnace is in the form of either a single-mode cavity or a multi-mode cavity operating at a fixed frequency. The single-mode cavity can generate a much higher intensity of EM field than the multi-mode cavity, therefore is more favorable for fast heating processes. Schematic of a typical single TE_{103} mode cavity resonator with a maximum power of 6 kW, used for heating SiC is shown in Fig. 1. Resonator was equipped with three different types of tuning mechanisms: (1) a three-stub tuner consisting of three movable screws positioned in a line on top of a waveguide just behind the iris, (2) a simple wheel device to increase or decrease the size of the iris, and (3) an adjustable back wall that can lengthen or shorten the resonator cavity; which allow the shape of the waveguide and resonator to be adjusted to maintain a

resonance condition. This provides the intense electric field necessary to attain very high temperatures with short ramp times. Encapsulated ion-implanted SiC samples or ion-implanted SiC samples encased in an amorphous SiC crucible are then placed inside another enclosure made of an insulator such as MgO to minimize radiative loss during heating. This entire assembly is mounted inside the resonator for heating. The amorphous SiC crucible minimizes sublimation from the uncapped implanted SiC surface by maintaining Si overpressure in the vicinity of implanted SiC sample during high-temperature heating. Further details of the system shown in Fig. 1 can be obtained from (Gardner et al., 1997). For the cavity resonator system described so far the heating ramp rate is 200 ^{o}C/min, with the implanted SiC samples encased in an amorphous SiC crucible (see Fig. 1(b)). Heating rates as high as 10-100 ^{o}C/s are achievable in single-mode cavity resonators with a reduced thermal mass. But, these rates are not enough for the present day ultra-fast heating rate requirements of Si, GaN and SiC device processing. In addition, there are a number of technical barriers for achieving very high heating rate with a single mode cavity. First, the use of a fixed frequency magnetron as microwave source leads to a mismatch in resonant frequencies between the microwave source and the loaded cavity since the characteristic frequency of the loaded cavity shifts as the temperature changes during the thermal process. Second, the cavity is mechanically tuned, so its response to coupling change is slow, limiting the maximum achievable heating rate. Third problem with the cavity coupling technique is arcing and the breakdown of plasma inside the cavity as the microwave power reaches the threshold level to breakdown the ambient gas in the cavity. Especially in the presence of conductive material, such as a metal, inside the cavity, the electric field is significantly enhanced at the edge of the conductive material, resulting in arcing at a much lower power level than that of the threshold of the ambient gas. The limitation of input power due to the arcing problem also limits the ability of cavity technique in achieving high heating temperatures and ultra-fast heating rates. Fourth limitation with the cavity heating technique is the limitation on the size of the load (semiconductor wafer), which must be smaller than the size of the cavity. This problem gets worse in single mode cavity, where the size of the cavity decreases with increasing operating frequency. These limitations of cavity microwave heating demand an alternative way of coupling microwaves to the materials to be heated, especially for ultra-fast and high-temperature heating applications. In present day nano-dimensional Si integrated circuit applications ultra-fast rapid thermal heating is required and in case of large dimensional SiC and GaN devices, both ultra-fast and high-temperature heating are desired.

3. Need for ultra-fast and/or high-temperature thermal processing of semiconductor devices

Ion-implantation is an indispensable technique for achieving planar selective area doping in fabricating SiC, GaN and ZnO high-power electronic and opto-electronic devices. Other doping methods such as thermal diffusion are impractical for the SiC, GaN and ZnO technologies because the diffusion coefficients of the technologically relevant dopants in these materials is very small (Sadow & Agarwal, 2004; Pearton et al., 2006), for example even at temperatures in excess of 1800 ^{o}C for SiC. For the current nano-dimensional Si technology also ion-implantation is the only selective area doping method available due to its precise control over the doping concentration and doping depth. However, ion-implantation process causes damage to the semiconductor crystal lattice and also the as-implanted

dopants do not reside in electrically active substitutional sites in the semiconductor lattice (Ghandhi, 1994). Therefore, the ion-implantation step always needs to be followed by a high-temperature annealing step for alleviating the implantation-induced lattice damage and for activating the implanted dopants (i.e. moving them from electrically inactive interstitial sites to the electrically active substitutional lattice sites).

For SiC, the implanted n-type dopants (nitrogen and phosphorus), depending on the implant dose, may require annealing temperatures up to 1900 ^{o}C, whereas implanted p-type dopants (aluminum and boron) may require temperatures in excess of 1900 ^{o}C (Seshadri et al.' 1998; Heera et al., 2004; Rambach et al., 2008). The higher annealing temperatures required for p-type dopants is a result of the higher activation energy required for forming the substitutional Al_{Si} acceptors compared to the P_{Si} donors. Also, the defects introduced by the Al implantation require higher annealing temperatures to be removed as opposed to the defects introduced by the P and N implantation (Seshadri et al. ,1998). Ultra-high temperature annealing not only helps to remove defects generated by the ion-implantation process but also the pre-existing defects in the material, which helps in obtaining a long ambipolar carrier lifetime in SiC p-i-n diodes (Jenny et al., 2006). Implanted p-type dopants (Mg) in GaN require annealing temperatures in excess of 1300 ^{o}C for satisfactorily removing implantation-induced defects, for activating the implanted dopants, and for recovering the luminescence properties (which are severely degraded by the ion-implantation) (Pearton et al., 2006; Feng 2006). A higher annealing temperature requirement for activating p-type implants compared to n-type implants in GaN is primarily due to the much larger formation energy of the substitutional Mg_{Ga} acceptors compared to the Si_{Ga} donors.

Traditionally, post-implantation annealing of SiC is performed in either resistively or inductively heated, high-temperature ceramic furnaces, since temperatures > 1600 ^{o}C are required. The furnaces used for annealing SiC have modest (few ^{o}C/s) heating and cooling rates, which makes annealing SiC at temperatures > 1500 ^{o}C using the traditional furnaces impractical because of an excessive SiC sublimation at such high temperatures when exposed for long durations. This problem can be alleviated to a certain extent by capping the SiC surface with a layer of graphite prior to annealing (Negoro et al., 2004; Vassilevski et al., 2005), but still the maximum conventional annealing temperatures are typically limited to about 1900 ^{o}C to preserve the surface integrity of SiC. For efficiently activating implanted p-type dopants in SiC and for removing the implantation-induced lattice defects, annealing temperatures > 1900 ^{o}C are required. In addition to the annealing temperature, the ramping rates also have an affect on the defect density and electrical characteristics of ion-implantation doped SiC (Poggi et al., 2006; Ottaviani, 2010). As for GaN, temperatures > 1300 ^{o}C are required for completely activating in-situ as well as ion-implanted p-type dopants. This is because of thermally stable defect complexes, which need temperatures as high as 1500 ^{o}C for breaking. However, when annealed at temperatures > 700 ^{o}C, GaN decomposes into Ga droplets due to nitrogen leaving the surface. This can be minimized by capping GaN with AlN. Annealing of GaN is performed in halogen lamp-based RTA systems, due to the rapid heating/cooling rates accorded by these RTA systems. However, due to their quartz hardware, these halogen lamp based RTA systems are limited to a maximum temperature of 1200 ^{o}C, which is not sufficient to effectively anneal p-type GaN. Laser annealing is known to result in high defect density and low implant activation for SiC (Ruksell and Ramirez, 2002; Tanaka et al., 2003), which is not suitable for achieving optimum device performance.

The conventional halogen lamp rapid thermal processing (RTP) technique, widely used in current Si device processing, is not suitable for future reduced size nano-dimensional devices due to its inability to reliably control annealing time to millisecond range (Tian, 2009), which is mandatory for future nm dimension Si devices for tight control of implant profiles. Millisecond range annealing method like laser annealing does not yield acceptable results for commercial production.

Based on what is presented above, raising the annealing temperature and reducing the temperature ramp-up and ramp-down rate are key elements in solving the most critical problems in the post-implantation annealing of both Si and large bandgap materials. Hence, for these two different device technologies, as shown in Fig. 2, the current annealing trend is either faster (for Si nano-devices) or both hotter and faster (for SiC, GaN and ZnO devices) compared to the existing annealing methods. Annealing temperatures as high as 2100 ^{o}C and temperature ramp-up and ramp-down rates as high as 2000 ^{o}C/s are desirable for these technologies.

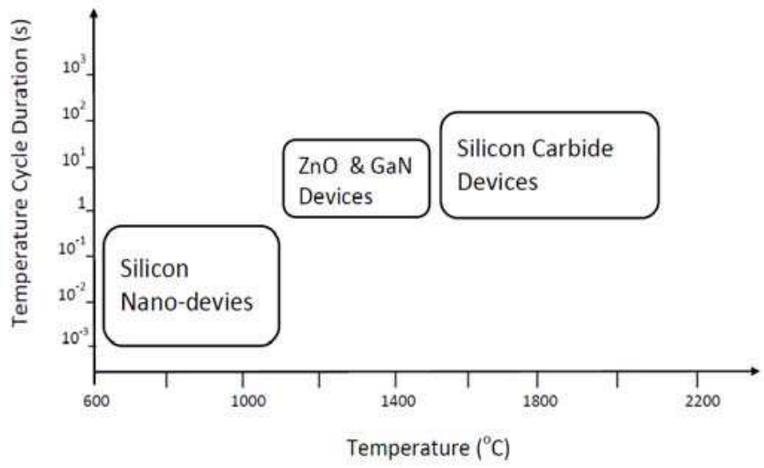

Fig. 2. Typical annealing temperature-time cycle requirements of different semiconductor device technologies.

One annealing method that satisfies the above requirements for both large bandgap and Si device applications is the solid-state microwave annealing (Sundaresan et al., 2007a, 2007b, 2008; Tian, 2009; Y. Tian & M.Y. Tian, 2009; Aluri et al., 2010). In this novel annealing method, microwaves coming from a microwave head are coupled to the sample directly. Microwave annealing provides ultra-fast heating and cooling rates and a good control over the annealing time when the semiconductor wafer is encased in microwave transparent materials. The heating rate is very high because the microwaves are absorbed only by the semiconductor wafer and not by the surroundings. The cooling rate is also high because the ambient surrounding the sample is not heated during the annealing process. Another attractive feature of microwave annealing is the selective heating of the doped region. Microwaves are absorbed more efficiently by the heavily doped region compared to the lightly doped regions in the same sample. Due to this reason, a heavily implantation doped region can be selectively annealed without adversely affecting the doping profile of lightly doped un-implanted region. This is possible because some of the implantation damage is recovered during ramp up transient, even before the sample reaches the annealing

temperature, increasing its conductivity to a higher level than the background pre-implant conductivity. The solid-state microwave annealing is different from above explained microwave cavity method used for annealing Si (Spinter et al., 1981; Scovell, 1984; Amada, 1987; Zhang et al., 1994) and SiC (Gardner et al., 1997) , where microwaves in a cavity resonator are coupled to the sample for heating. The microwave cavity resonators require mechanical tuning and operate at a fixed resonant frequency, which compromise their efficiency and suitability for batch processing. The new solid-state microwave annealing method does not involve any cavity and has favorable features such as variable operating frequency, swift electronic tuning and other automation capabilities, which make it suitable for commercial mass semiconductor device production application.

4. Ultra-fast solid-state microwave annealing

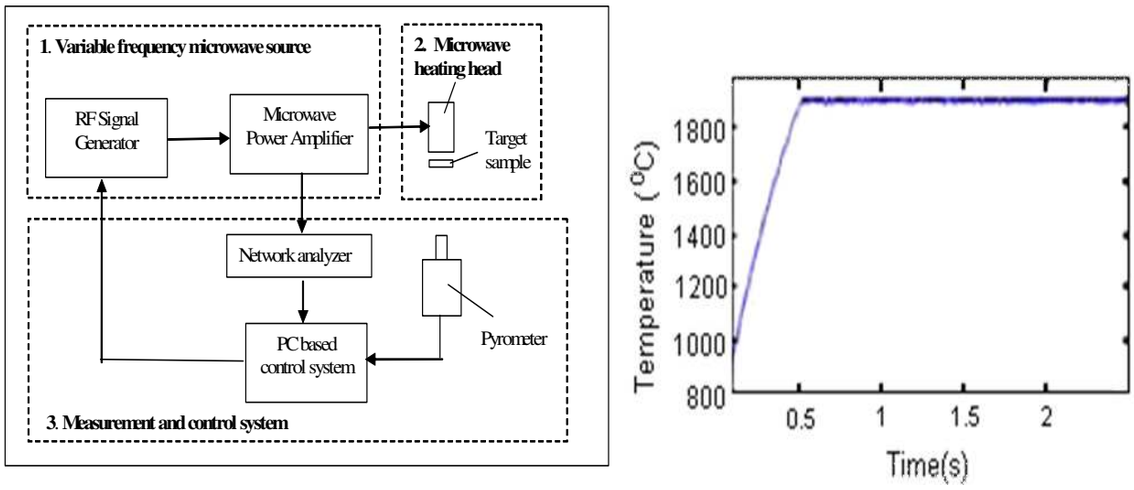

(a) (b)

Fig. 3. (a) Block diagram (adapted from Tian, 2009) and (b) a typical temperature-time cycle profile, of a solid-state microwave annealing set-up.

Recently there is a rapid advancement of solid state microwave techniques for mobile phone and wireless communication application. Seizing this opportunity, LT Technologies (LTT) has developed a unique solid-state microwave Rapid Thermal Processing(RTP) system. Figure 3(a) shows the block diagram of the LTT's solid-state microwave RTP system. This microwave RTP unit can be divided into three main parts: (1) a variable frequency microwave power source which consists of a RF signal generator and a RF power amplifier, (2) a microwave heating head which is closely placed on the top of the target sample and couples microwave energy to the target, and (3) a measurement and control system which consists of a network analyzer, a PC based control system and an optical pyrometer. The use of a variable frequency microwave source, instead of a fixed frequency magnetron, allows a broad bandwidth in the selection of a suitable operating frequency. It also provides the flexibility of sweeping the source frequency during the thermal process to compensate for the characteristic frequency shifting due to the temperature change of the specimen. In addition, the variable frequency source has the capability of generating pulsed or modulated microwave power for optimal energy dissipation. This solid state, cavity-less

and variable frequency based microwave technology is capable of generating high-power, short-duration, spatially uniform, and material-specific microwave pulses. It offers many novel features and desirable characteristics for rapid thermal processing of compound semiconductors and other advanced materials at very high temperature. These novel features include: (1) very high heating temperature (> 2000 ^{o}C), (2)ultra-fast ramping rate (up to 2000 ^{o}C/s), (3) automation (a PC based computer control) to regulate the temperature uniformity and stability, and (4) scalability of the system to accommodate technology changes such as device feature size shrinkage and wafer size increase (Y. Tian and M.Y. Tian, 2009; Tian, 2009; Sundaresan et al., 2007b).

For SiC sample heating, the microwave power generated by the variable frequency power source is amplified and then coupled to the SiC sample through the heating head. The sample temperature is monitored by an infrared pyrometer. The SiC and GaN sample emissivities were both measured as 0.8 using a blackbody source and this emissivity value was keyed into the pyrometer for all temperature measurements. The microwave system can be tuned to efficiently heat semiconductor samples at variable frequencies. Since the samples are placed in an enclosure made of microwave transparent, high-temperature stable ceramics such as boron nitride and mullite, microwaves only heat the strong microwave absorbing (electrically conductive) semiconducting films, which present a very low thermal mass in comparison with a conventional furnace where the surroundings of the sample are also heated. Thus, heating rates > 1000 ^{o}C/s are possible. In fact, selective heating of thin, highly doped semiconductor layers is possible if the doped layers are formed on semi-insulating or insulating substrates. For efficient microwave annealing of implanted semi-insulating (SI) SiC substrates and GaN epilayers grown on (electrically insulating) sapphire substrates, placing a heavily doped 4H-SiC wafer as a susceptor in close proximity to the sample to be annealed is desired. It is possible to directly couple microwave power and heat GaN epilayers grown on sapphire, without using any susceptor. However, the spatial distribution of temperature across the sample in general is non-uniform. Placing a SiC susceptor sample underneath the GaN sample of interest solves this problem.

A typical temperature profile for microwave heating of a 4H-SiC sample is shown in Fig. 3(b). It can be seen that the high temperature of 1900 ^{o}C is reached within 0.5 second and the temperature oscillation is less than 10 ^{o}C. For microwave RTP of a large wafer, an array of microwave heating heads is placed on top of the wafer. The number of heating heads can be changed depending on the size of the wafer and the requirement of temperature uniformity across the wafer. Multiple microwave power sources and multiple temperature sensors are required to run and monitor the rapid thermal process effectively. Solid-state microwave heating is advantageous for high-temperature processing of wide bandgap semiconductors such as SiC, GaN and ZnO. The microwave heating system has a capability to reach sample temperatures > 2000 ^{o}C (for SiC wafers) with heating and cooling rates in excess of 1000 ^{o}C /s.

5. Microwave heating for synthesizing SiC nanowires

Over the past decade, one dimensional (1-D) semiconductor nanostructures, such as nanotubes and nanowires, have attracted special attention due to their high aspect and surface to volume ratios, small radius of curvature of their tips, absence of 3-D growth related defects such as threading dislocations, and fundamentally new electronic properties resulting from quantum confinement. These nanostructures are expected to play a crucial role as building blocks for future nanoscale electronic devices and nano-electro-mechanica-

systems (NEMS), designed using a bottom-up approach. The 1D and quasi-1D nanowires of Si, GaN, ZnO, SiC and other semiconductors have been synthesized (Huang and Lieber, 2004; Law et al., 2004; Andrievski, 2009; Fang et al., 2010). Silicon carbide, due to its wide bandgap, high electric breakdown field, mechanical hardness, and chemical inertness, offers exciting opportunities in fabricating nanoelectronic devices for chemical/biochemical sensing, for high-temperature, for high-frequency and for aggressive environment applications (Fan et al., 2006). Several techniques have been applied to synthesize SiC nanowires using physical evaporation, chemical vapor deposition, laser ablation, and various other techniques (Sundaresan et al., 2007c). A simple and cheaper method to grow SiC nanowires is highly desirable. A sublimation-sandwich method utilizing microwave heating satisfies this requirement.

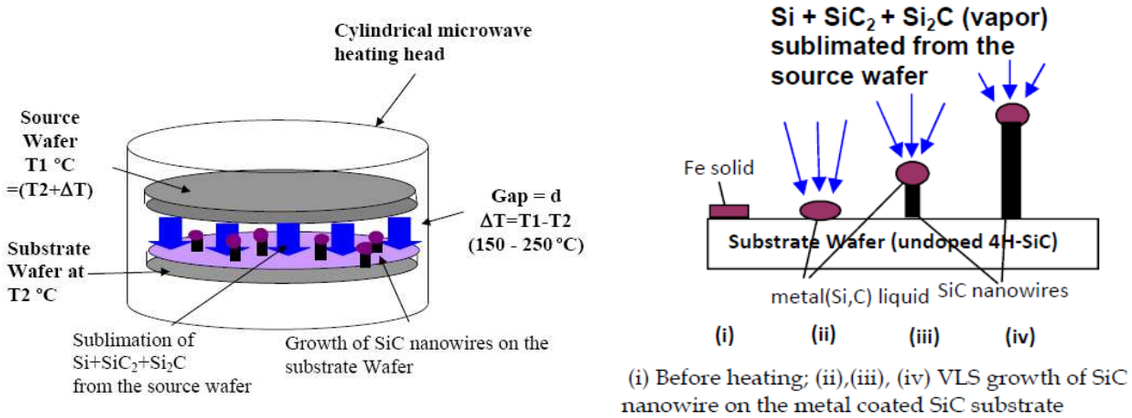

(a) (b)

Fig. 4. Schematics of (a) sandwich cell used for SiC nanowire growth, and (b) SiC nanowire growth process.

Schematic of a typical "sandwich" cell used for SiC nanowire growth is shown in Fig. 4(a). The 'sandwich cell' in Fig. 4 consists of two parallel 4H-SiC wafers with a very small gap, 'd', between them. The bottom wafer in Fig. 4(a) is semi-insulating SiC, which will be referred to as the 'substrate wafer' hereafter. The inner surface of the substrate wafer is coated with a 5 nm layer of Fe, Ni, Pd, or Pt that acts as a catalyst for the vapor-liquid-solid (VLS) growth of SiC nanowires. The top wafer in Fig. 4(a) is a heavily n-type (nitrogen doped) in-situ doped SiC, which will be referred to as the 'source wafer'. As shown in Fig. 4(a), the microwave heating head is placed around the sandwich cell. Due to the difference in electrical conductivity of the source wafer and the substrate wafer, at a given microwave power, the source wafer temperature is higher than the substrate wafer temperature, resulting in a temperature gradient, ΔT, between the two wafers. When the Si- and C-containing species, such as Si, SiC_2, and Si_2C sublimate from the source wafer at temperatures > 1500 °C, the temperature gradient (ΔT) provides the driving force for transporting these species to the substrate wafer. On the substrate wafer surface, the metal film is either already molten at the growth temperature, or it melts after absorbing the Si species and forms spherical islands to minimize its surface free energy. The Si- and C-containing vapor species are absorbed by these metal islands, converting them into liquid droplets of metal-Si-C alloys. As shown in Fig. 4(b), once this alloy reaches a saturation point for SiC, a precipitation of SiC occurs at the liquid-substrate interface thereby leading to

a VLS growth of the SiC nanowires. The nanowires always terminate in hemispherical metal-Si alloy end-caps. While group VIII metals facilitate growth of SiC nanowires, Au is not suitable as a catalyst in this VLS process due to its possible evaporation at the growth temperature.

The sublimation sandwich method described above can reliably grow SiC nanostructures with predictable morphologies, with very high growth rates. Since, the sublimation sandwich method is widely used in industry for growing SiC epilayers and substrates, there exists a vast body of information for controlling the polytype, doping, orientation, etc. of the SiC growth. The sandwich cell described above is a nearly closed system because of the small gap between the source and substrate wafers, which allows precise control of the composition of the vapor phase in the growth cell. At the same time, the system is open to the species exchange between the sandwich growth cell and the surrounding environment in the chamber. By appropriately adjusting the composition of the precursor species in the vapor, this approach has the potential to control the doping levels, or create heterostructures in the growing nanostructures. Another important feature of the sandwich growth cell is its compact size, which significantly reduces the volume of the surrounding chamber. The use of a small chamber not only saves the cost by utilization of small amount of expensive source materials, but also significantly reduces the vacuum pumping cycle time, which is needed for a high throughput fabrication. Yet another novel feature is the dynamic range of temperature ramping rates (≥ 1000 ^{o}C/s) that are possible using the microwave heating system. This is another process parameter which can be tweaked to circumvent some thermodynamic restrictions.

6. Organization of rest of the chapter

In the rest of the chapter, results on the application of microwave annealing: to activate ion-implanted dopants in SiC, to activate in-situ doped and ion-implantated dopants in GaN, to grow SiC nanowires, and for other possible usages in device processing are presented. Unless otherwise specified, the phrase 'microwave annealing' hereafter refers to solid-state microwave head based annealing. The Polytype of SiC used for the solid-state microwave head based annealing was 4H. Wherever appropriate results of microwave cavity annealing on ion-implanted 6H-SiC are also presented. Implant activation behavior is similar for both 4H and 6H polytypes of SiC. The GaN results are for layers grown on sapphire substrate.

For brevity complete information on ion-implantation schedules are not provided, but the readers are referred to publications where this information is provided. In case of SiC, except for boron, for all other species, multiple-energy ion-implantations were performed to obtain a uniform implant concentration over a specific thickness from the surface of the wafer. Results are provided on the basis of volumetric concentration of the implant. Surface roughness, structural and electrical properties of: aluminum, boron, nitrogen and phosphorus implanted SiC, and magnesium ion-implantation (or in-situ) doped GaN, subjected to ultra-fast solid-state microwave annealing (or cavity microwave annealing) at temperatures in the range of 1300 ^{o}C – 2120 ^{o}C are presented.

7. Surface roughness of microwave annealed SiC and GaN

For high-yield device production the surface roughness of the heat-treated semiconductor should be close to the pre-annealed value. In case of conventional furnace annealed

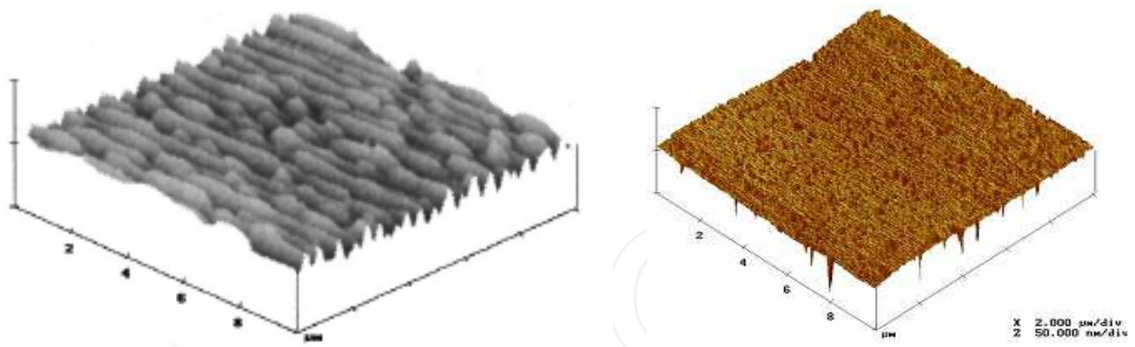

(a) (b)

Fig. 5. Tapping mode AFM images of: (a) implanted SiC annealed by conventional furnace at 1600 ^{o}C for 10 min without cap and (b) implanted GaN annealed by microwaves with AlN cap at 1500 ^{o}C for15 s

implanted SiC the surface becomes rough due to continuous long furrows running in one direction across the sample surface (see Fig. 5(a)). These furrows are supposed to be caused by the thermal desorption of species such as Si, SiC_2, Si_2C, etc, a mechanism which is popularly known as 'step bunching' (Capano et al., 1999; Rao et al., 1999; Vathulya and White, 2000; Rambach et al., 2005). The step bunching puts fabrication constraints on SiC devices (Phelps et al., 2002). The step bunching is observed not only on uncapped furnace annealed SiC but also on epitaxial layers grown on off-axis cut SiC wafers. The step bunching related surface roughness can be decreased considerably by chemical mechanical polishing (Kato et al., 2010). For uncapped ion-implanted SiC samples microwave annealed in open air at temperatures ≤ 1850 ^{o}C, using another SiC piece proximity (in order to suppress Si sublimation during annealing), deep furrows are not formed and the surface roughness measured by tapping mode AFM measurements is ≤ 2 nm. The roughness increased quickly for higher annealing temperatures reaching a value of 8.5 nm for annealing at 1975 ^{o}C (Sundaresan et al., 2007a). Parabolic oxide growth on SiC sample surface was observed for open air microwave annealing. To prevent oxide growth, the microwave anneals need to be performed in a controlled inert atmosphere of N_2, Ar, or Xe. Arching due to breakdown of gas was observed for all inert gases except for the N_2. Due to this reason, N_2 is the preferred ambient for microwave annealing of SiC and GaN. In case of GaN, N_2 also provides nitrogen over-pressure to minimize nitrogen sublimation from the GaN surface during annealing, though it is not effective at normal pressures. High temperature microwave annealing in N_2 ambient not only prevents oxidation of the SiC surface during annealing but also results in a reduction of surface roughness. For SiC samples annealed in the N_2 ambient, without any deposited encapsulant (but with the SiC proximity), the RMS surface roughness after annealing at 2050 ^{o}C for 30 s is only about 2 nm (Sundaresan et al., 2007b). Microwave annealing without any deposited encapsulation resulted in severe sublimation of the implanted sample surface even though the surface roughness is low. The sublimated layer thickness for microwave annealing at 2050 ^{o}C for 30 s is about 120 nm, which is a substantial part of the implanted layer thickness. To prevent sublimation of this magnitude, a graphite cap formed by heat-treatment of a deposited photoresist layer is required (Vassilevski et al., 2005; Rao et al., 2010). Surface roughness of graphite cap protected microwave annealed samples is comparable to that of as-implanted/un-annealed samples (Sundaresan et al., 2008).

High-temperature microwave annealing of GaN results in a very rough (≥ 10nm) surface with formation of hexagonal cavities, due to sublimation (Aluri et al., 2010; Sundaresan et al., 2007d). It is well known that nitrogen sublimates from GaN even at annealing temperatures as low as 700 ^{o}C, but temperatures as high as 1500 ^{o}C are required for activating ion-implanted Mg acceptors in GaN. Protecting GaN from sublimation even with deposited capping layers is not easy. It is quite tempting to use graphite cap, which successfully protected SiC surface during high-temperature microwave annealing, for the GaN also. Unfortunately, the graphite cap is ineffective in protecting GaN surface at annealing temperatures > 1000 ^{o}C, presumably because of the stress at the GaN/graphite interface. In general, capping layers having a good lattice matching with the semiconductor layer they are supposed to protect are more effective in withstanding high annealing temperatures. The MgO capping layer (200 nm thick), formed by e-beam evaporation, and having 6.5% lattice mismatch with GaN, could protect GaN only up to a microwave annealing temperature of 1300 ^{o}C (Sundaresan et al., 2007d). Pulsed-laser-deposited AlN(600 nm thick), having a 2.6% lattice mismatch with GaN, protects GaN layers reasonably well up to microwave annealing temperatures as high as 1500 ^{o}C (Sundaresan et al., 20007; Aluri et al., 2010). Surface roughness of AlN capped GaN is comparable to that of a virgin sample for 5s annealing but increases with increasing annealing time at 1500 ^{o}C (see Fig. 5(b) for 15 s anneal at 1500 ^{o}C). For additional protection, the AlN encapsulated GaN sample should be placed face down on the polished SiC susceptor substrate during annealing.

8. Thermal stability of implants in microwave annealed SiC and GaN

It is well known that dopants such as N, Al and P are thermally stable in SiC. No redistribution of these impurities was observed either in long duration conventional furnace annealed samples or in samples annealed by microwaves (for both microwave cavity and solid-state microwave head methods) even at temperatures as high as 2100 ^{o}C. On the other hand, the boron implant is known to redistribute in SiC even for low-temperature annealing, especially if the implant is a shallow implant. For the 50 keV boron implant, the 1670 ^{o}C / 10 s microwave annealing resulted in a substantial out-diffusion of boron from the SiC surface. The small atomic size of boron, resulting in a high transient enhanced diffusion (TED), is believed to be responsible for this behavior. However, for the completely buried 1 MeV boron implant, the 1670 ^{o}C / 10 s microwave annealing did not result in any significant boron redistribution (not shown). Boron atom density depth profiles obtained by SIMS measurements on 200 keV/1×10^{15} cm^{-2} B implanted SiC are shown in Fig. 6, before and after microwave and furnace annealing. The boron implant out- diffusion front in Fig. 6 probably is caused by the segregation of boron towards ~ 0.7 Rp, the depth where implant lattice damage is at its maximum. This is caused by the lattice strain at this location. A similar feature was observed in the B- depth profiles of 1 MeV/ 2 x 10^{15} cm^{-2} B for 1670 ^{o}C / 10 s microwave annealing. Out-diffusion of the boron is less for the microwave annealing compared to the furnace annealing even though the microwave annealing was performed at a temperature 270 ^{o}C higher than the furnace annealing. This again establishes the attractiveness of ultra-fast solid-state microwave annealing compared to the furnace annealing, which has much slower heating and cooling rates. Thus, the ultra-fast microwave annealing is reasonably effective in maintaining the integrity of buried boron implant profiles, but a substantial boron out-diffusion is still observed for 10 s microwave annealing at 1670 ^{o}C, for low-energy B ion implantation, where the implant profile is very close to the surface.

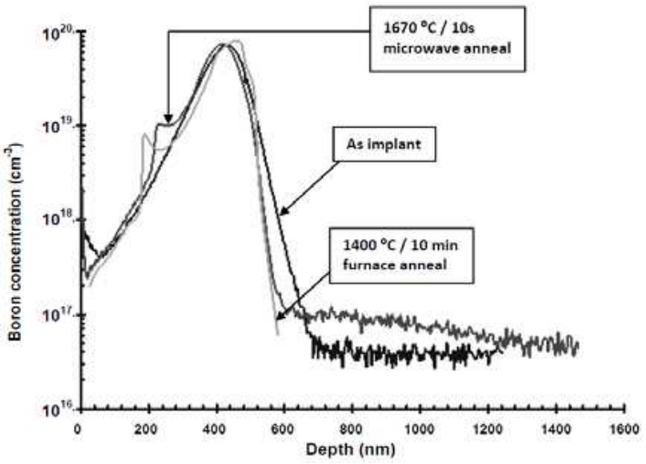

Fig. 6. SIMS depth profiles of 200 keV/1×10^{15} cm^{-2} B^{+} implant in SiC before and after anneal.

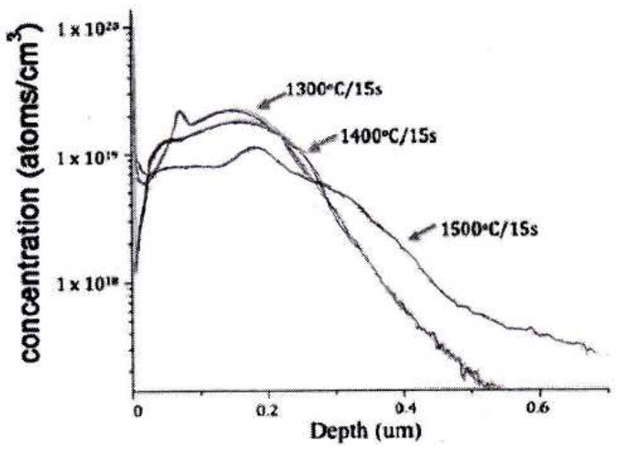

Fig. 7. SIMS depth profiles of 150 keV/5×10^{14} cm^{-2} Mg-implanted GaN after 15s microwave annealing at different temperatures.

The out-diffusion of the implant, as seen for the B-implant in SiC, is observed for Mg implant in GaN also. In addition, a significant in-diffusion of the Mg implant, as shown in Fig. 7, can be seen. The fast out-diffusion and in-diffusion of Mg in GaN at high annealing temperatures is due to a high diffusion coefficient of acceptors in III-V compounds. The extracted Mg implant doses in microwave annealed GaN samples are slightly lower compared to the extracted dose in the as-implanted GaN material due to out-diffusion of Mg into the deposited AlN cap during microwave annealing (Aluri et al, 2010). Despite of the out- and in-diffusion of the Mg implant during annealing, the implant profiles are reasonably stable at least up to a microwave annealing temperature of 1400 ^{o}C.

9. Lattice perfection of microwave annealed ion-implanted SiC and GaN

An effective annealing process removes all defects introduced in the material by the ion-implantation doping step. In case of SiC, Rutherford back-scattering (RBS) yield in ion-implanted microwave annealed samples is below that of the conventional furnace annealed samples indicating a better lattice quality for the ultra-fast microwave annealed samples. As

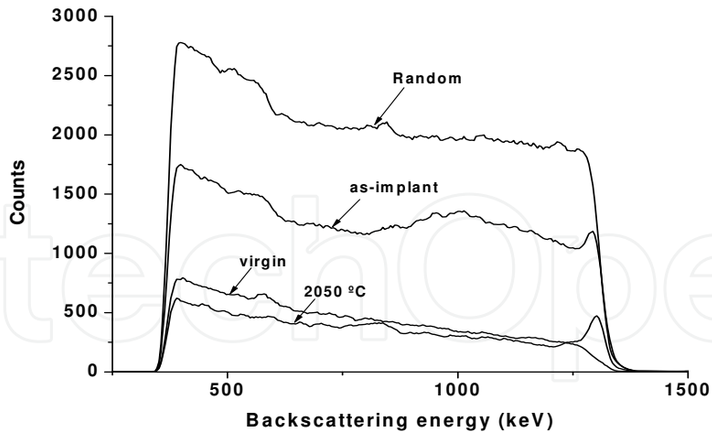

Fig. 8. RBS-C aligned spectra on multiple energy Al ion-implanted 4H-SiC, before and after 2050 °C/15 s microwave annealing. Random and aligned spectra on the virgin sample are also shown for comparison.

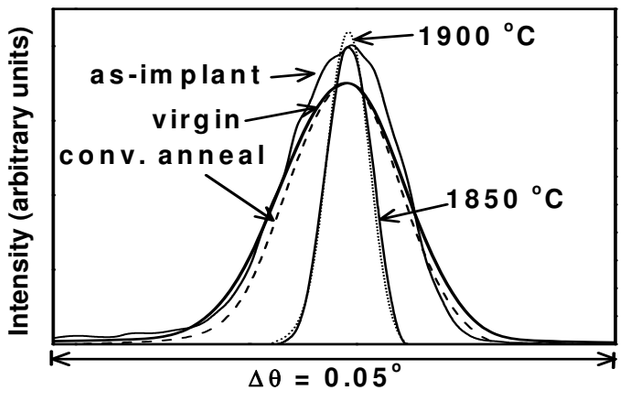

Fig. 9. X-ray rocking curves of the SiC (004) from the Al ion-implanted 4H-SiC, before and after 30 s microwave annealing. For comparison, curves on virgin and 1800 °C/5 min. conventional furnace annealed samples are also shown.

shown in Fig. 8 for aluminum ion-implanted 4H-SiC, the aligned RBS yield in the implanted ultra-fast microwave head annealed material is even below the aligned virgin level. The ultra high-temperature microwave annealing is very effective in removing not only the defects introduced by the ion-implantation step, but also the native defects present in the material before the ion-implantation step. This conclusion is based not only on the results of RBS via channeling (RBS-C) measurements but also the x-ray rocking curve measurements on the as-implanted, microwave annealed and virgin samples. The full-width-at-half-maximum (FWHM) of the high resolution x-ray rocking curves for the SiC (004) reflection of the microwave annealed Al-implanted SiC sample is below that of the virgin sample (see Fig. 9). The FWHM of the sample microwave annealed at 1900 °C for 30s is 15 arc-sec compared to the value of 22 arc-sec in the virgin sample. The x-rays penetrate much deeper (about 3 μm under dynamical diffraction condition) than the implanted region depth (0.3 μm) and hence probe the un-implanted region below the implanted surface region as well,

which confirms the removal of defects in this region also (Mahadik et al., 2009). Microwave annealing on unimplanted SiC sample did not result in any reduction in defect density. It is speculated that the defects such as carbon interstitials (C_i) created by the ion-implantation process diffuse from the implanted surface region into the un-implanted bulk below the implanted region, annihilating native defects such as carbon vacancies (V_C) in the bulk region during the annealing process (Storasta and Tsuchida, 2007). It means preexistence of implantation process created defects in the surface region is required for reducing defect density in the bulk underneath during annealing. In case of microwave cavity annealing, for comparable annealing temperatures, the RBS yield of microwave annealed sample is similar to that of a conventional furnace annealed sample. So, the combination of ultra-fast temperature ramping rate (which is not high for microwave cavity annealing) and the very-high annealing temperature associated with the solid-state microwave head annealing are the contributing factors for reducing the defect density below the virgin level.

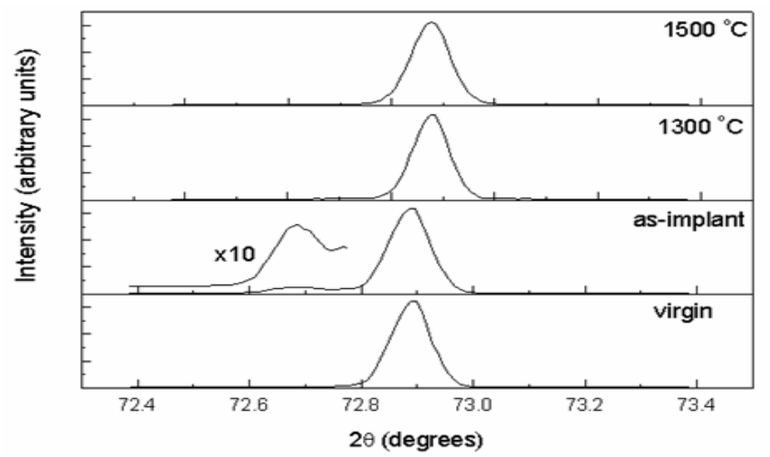

Fig. 10. X-ray diffraction scans of the GaN (004) for Mg-implanted GaN, before and after 15 s microwave annealing. For comparison a scan on the virgin sample is also shown.

Figure 10 shows the XRD scans of the GaN (004) reflections of the as-grown, as-implanted, and 15 s time duration microwave annealed 150 keV/5 $\times 10^{14}$ cm^{-2} Mg-implanted GaN samples. It can be seen that the as-implanted sample has the defect sublattice peak, which is due to the interference of the x-rays from the implanted impurity in the interstitial sites. The defect sublattice peak disappears after microwave annealing, confirming that the implanted Mg has moved to electrically and optically active substitutional lattice positions. In addition, the FWHM value of the GaN (004) peak also decreases upon annealing (from 310 arc-sec before annealing to 273 arc-sec after 1300 ^oC annealing), indicating that the implant induced damage (which is in the form of Ga and N interstitials) has been removed. It can be seen that upon 1300 °C/15 s annealing, the FWHM value decreased to below the virgin sample level (293 arc-sec). The FWHM value goes down even further for higher temperature anneals (252 arc-sec for 1500 ^oC annealing), reaching values much lower than that of the unimplanted (virgin) sample. This observation is consistent with the results of ion-implanted SiC. This suggests that the high-temperature microwave annealing process may remove some of the growth related defects in the unimplanted region of GaN films, improving their crystalline quality. This is not surprising, considering that the GaN films growth temperatures are way below the microwave annealing temperatures. However, this does not necessarily mean that

there are no point defects left in microwave annealed Mg-implanted GaN. The electrical measurements on Mg-implanted microwave annealed material indicated the presence of residual defects with donor type behavior even after 1500 ^{o}C annealing for 15 s. In case of multiple-energy Mg-implanted GaN, the implantation damage created sublattice peak in XRD remained even after 1500 ^{o}C annealing (Aluri et al., 2010). In case of in-situ Mg doped GaN, microwave annealing at 1500 ^{o}C resulted in breaking of defect complexes, which have a deep donor behavior (Sundaresan et al., 2007d).

10. Electrical characteristics of microwave annealed ion-implanted SiC and GaN

Nitrogen and phosphorus are the most widely used donor (n-type) impurities in SiC. Phosphorus is a preferred donor dopant in SiC because of its higher solubility limit in SiC than that of nitrogen, which cannot be incorporated in excess of 3×10^{19} cm^{-3} due to precipitation during post-implantation annealing. For donor doping concentrations of $\leq 1\times10^{19}$ cm^{-3} either nitrogen or phosphorus implants can be used. But, for higher doping concentrations the phosphorus is the only viable donor dopant in SiC. Resistivity is an important material property that can be used to evaluate the electrical characteristics of an implanted layer, because a low resistivity is obtained only if both the implant electrical activation and the carrier mobility are high. Hence, room-temperature electrical resistivity is used as the prime figure of merit of the electrical characteristics of the microwave annealed implanted SiC layers. For a 170 ^{o}C higher temperature microwave annealing on nitrogen implanted SiC, the room-temperature electrical resistivity is 40% lower compared to the conventional furnace annealing at 1600 ^{o}C (Sundaresan et al., 2007a). Reduction of this magnitude in electrical resistivity is primarily obtained by a higher nitrogen implant substitutional activation (without sacrificing carrier mobility) in microwave annealed material compared to the conventional furnace annealed material.

The electrical resistivity of phosphorus implanted SiC material is more sensitive to the annealing temperature than the annealing duration (Sundaresan et al., 2007b). For 30 s time duration microwave anneals performed on 2×10^{20} cm^{-3} P^{+}-implanted 4H-SiC, with sample surface not protected by a graphite cap, the room-temperature electrical resistivity of the implanted layer dropped by 15 fold with an increase in annealing temperature from 1700°C to 1950°C. The electrical resistivity drop did not show any tendency towards minimum resistivity saturation even at 1950°C. While the initial decrease in electrical resistivity with increasing annealing temperature up to 1800°C is due to increasing substitutional electrical activation of the P donor, the later decrease at higher annealing temperatures is due to an increase in both P implant activation and carrier mobility, μ. The μ value tripled and the implant activation doubled with an increase in annealing temperature from 1800°C to 1950°C (Sundaresan et al., 2007b). High carrier mobilities are measured in microwave annealed samples due to not only the effective removal of implant lattice damage in the implanted region but also the removal of intrinsic lattice defects that existed in the pre-implanted material. Based on the results of this initial microwave annealing study on 2×10^{20} cm^{-3} P implanted 4H-SiC (only up to an annealing temperature of 1950 °C), during the later work on four other P concentrations; 5×10^{19} cm^{-3}, 1×10^{20} cm^{-3}, 4×10^{20} cm^{-3}, and 8×10^{20} cm^{-3}; the annealing temperature range was extended up to 2050°C, for the 30 s time duration anneals. The graphite cap enabled annealing at such high temperatures. The main reason for selecting higher annealing temperatures when compared to the initial study on 2×10^{20} cm^{-3} P

implanted material is the non-saturation of the electrical resistivity in the 2×10^{20} cm^{-3} P implanted material, even at an annealing temperature of 1950°C. In addition, higher implant concentrations like 4×10^{20} cm^{-3} and 8×10^{20} cm^{-3} are expected to require higher annealing temperatures than the 2×10^{20} cm^{-3} P implant concentration, due to a higher degree of implant damage in the material for these implant concentrations. For the P implant concentrations: 1×10^{20} cm^{-3}, 4×10^{20} cm^{-3}, and 8×10^{20} cm^{-3}, there is an additional 25% - 30% reduction in the room-temperature electrical resistivity of the implanted region for higher annealing temperatures compared to the value for 1950°C annealing. For a given phosphorus doping concentration, saturation of the minimum obtainable room-temperature electrical resistivity for microwave annealing seems to occur at around an annealing temperature of 2050°C. Variation of implanted layer room-temperature electrical resistivity

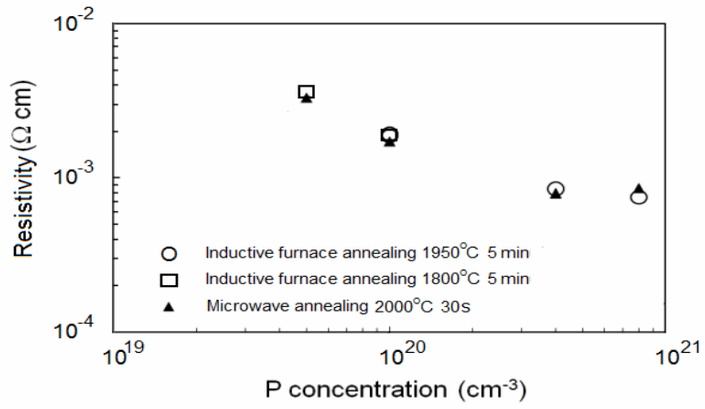

Fig. 11. Variation of measured room-temperature electrical resistivity with phosphorus implant concentration, in microwave annealed and conventional inductive heating furnace annealed 4H-SiC.

with the P-implant concentration for the 2000°C/30 s microwave annealing is shown in Fig. 11. For comparison, results of the conventional inductive heating furnace anneals are also shown in Fig. 11. The measured electrical resistivity data shows in general a lower resistivity values in microwave annealed material compared to the inductive furnace annealed material. A tendency towards saturation in the minimum obtainable resistivity is observed at around 6×10^{-4} Ω-cm, which is the lowest value reported to date on ion-implanted 4H-SiC. As far as resistivity is concerned, it seems, there is no appreciable benefit in going for P implant concentrations > 4×10^{20} cm^{-3}.

Aluminum has a lower acceptor ionization energy compared to the other acceptor impurities such as boron, gallium and indium (Handy et al., 2000). Due to this reason, Al is widely used for obtaining heavily doped p-type regions in SiC. Plots of room temperature sheet resistance (product of electrical resistivity and implant depth) and hole mobility, as a function of the microwave annealing temperature in the range 1750 ^{o}C – 1900 ^{o}C, for an anneal duration of 30 s, are shown in Fig. 12 for 1×10^{20} cm^{-3} Al implant to a depth of ~ 0.3 μm. It can be seen from Fig. 12 that increasing the microwave annealing temperature steadily lowers the sheet resistance, while increasing the hole mobility after an initial dip. Hole mobility in ion-implanted 4H-SiC is primarily controlled by scattering at ionized impurities and scattering at implantation-induced defects. The initial decrease in hole mobility (in Fig. 12) can be attributed to increased ionized Al impurity scattering. The later

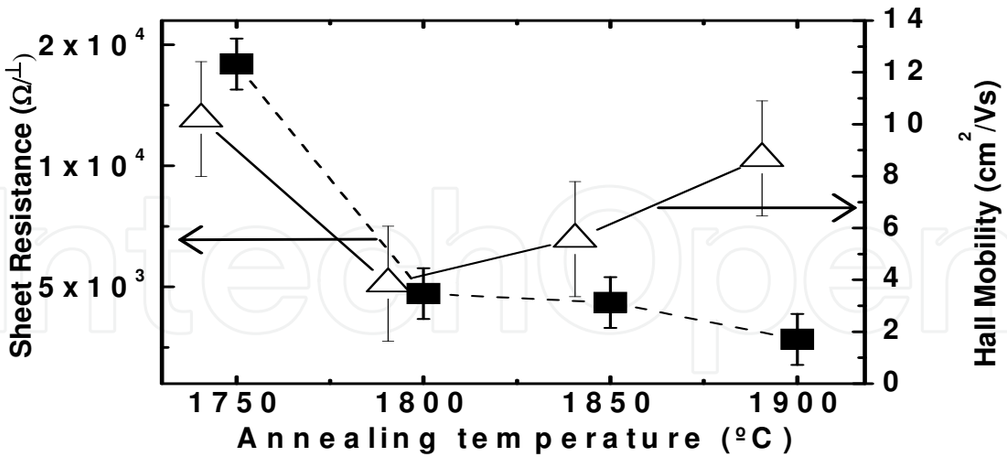

Fig. 12. Variation of measured room-temperature sheet resistance and hole mobility with annealing temperature for 30 s time duration microwave anneals.

increase in hole mobility with increasing temperature could be due to more effective defect removal by the microwave annealing. The measured room temperature sheet resistance (2.8 kΩ/□) for the 1900 ºC/30 s microwave annealed sample is a factor of 4.6 times lower compared to the value of 13 kΩ/□ measured for the 1800 ºC/5 min conventionally annealed sample, whereas the measured room temperature sheet carrier concentration (product of volumetric carrier concentration and implant depth, which is not shown) for the microwave annealed sample is almost one order of magnitude higher (3.2×10^{14} cm^{-2}) compared to the conventionally annealed sample (3.5×10^{13} cm^{-2}). But, the room temperature hole mobility for the microwave annealed sample is only about 40% lower than that for the conventionally annealed sample (9 $cm^2/V.s$ vs. 14 $cm^2/V.s$), even though the holes in the microwave annealed material are subjected to a much higher ionized impurity scattering than in the conventionally annealed sample. This means that the decreased sheet resistance measured for the microwave annealed samples is due to a combination of a much more effective Al implant activation, as well as effective implant-induced damage annealing, compared to the conventional furnace annealing.

The electrical characteristics of the microwave cavity annealed material are comparable to the conventional furnace annealed material for similar annealing temperatures (Gardner et al., 1997), again confirming that it is not microwaves that contribute to the favorable electrical characteristics, but the annealing temperature and the temperature ramping rates associated with the microwave head annealing. The temperature ramping rate also has a profound effect on the electrical characteristics of the annealed material (Poggi et al., 2006). Higher ramping rates associated with the solid-state microwave head annealing compared to the microwave cavity annealing are helpful in achieving better electrical properties in implanted material.

Single-energy (150 keV) magnesium ion implanted GaN protected by the AlN cap did not show any electrical conduction for microwave annealing temperatures < 1300°C and also for annealing durations <10 s (Aluri et al., 2010). The material remained highly resistive, with no breakdown voltage seen in two-probe current–voltage (I-V) measurements. The two-probe I-V measurements indicated decreasing breakdown voltage with increasing annealing temperature for 15 s duration anneals performed at temperatures ≥ 1300°C. But, variable

temperature van der Pauw–Hall measurements up to 200 °C on these samples did not show a consistent p-type behavior. While the sample showed a low p-type conductivity in one measurement, it showed an opposite type conductivity when the Hall measurements were repeated on the same sample at the same temperature. This could be due to close compensation between the Mg-acceptors which have a high ionization energy (≥ 200 meV) and the donor levels introduced in the material due to the implantation and annealing processes. Though the 15 s annealing is better than the 5 s annealing in decreasing the implant damage, a low residual implant damage in the form of point defects and defect complexes may still exist in the material, below the detectable level of the x-ray measurements. Some of the defect complexes have a deep donor behavior in GaN. In addition, it is well known that nitrogen vacancies have a donor behavior in GaN. Compensation of substitutional Mg acceptors by such donor levels limits the measurable net acceptor carrier concentration by the electrical methods; but, the photoluminescence (PL) measurements, which have no such limitation showed a Mg acceptor related donor-acceptor pair transition peak (Aluri et al., 2010). Hence, based on the XRD, PL, and I-V measurements it can be stated that the single-energy Mg-implanted films, after 15 s high temperature (≥ 1400 °C) microwave annealing have shown improved crystalline quality and acceptor activation of the Mg implant. But, the net Mg-acceptor activation seems to be compromised by compensating background donor defects left in the material even after 1500 °C/15 s annealing. The situation is much worse for multiple-energy Mg ion-implanted GaN. The microwave annealing couldn't remove the ion-implantation damage and hence the material remained highly resistive even after 1500 °C/15 s microwave annealing. Even in case of in-situ Mg doped GaN, microwave annealing at 1500 °C resulted in a decrease in compensating deep donor concentration and a consequent net Mg acceptor activation (Sundaresan et al., 2007d).

11. Results of differential microwave heating sublimation-sandwich method for growing SiC nano-structures

A schematic of the differential microwave heating sublimation sandwitch cell is already shown in Fig. 4. The substrate wafer temperature window for growing SiC nanostructures is 1550 °C to 1750 °C. In this growth method, the precursor Si and C containing species sublimate from the source wafer. Significant sublimation of Si and C species from a SiC wafer requires temperatures > 1400 °C (at 1 atm pressure). Therefore, the growth temperatures required for microwave heating sublimation sandwich method are higher than those typically employed for SiC nanowire growth (1000 °C – 1200 °C), since the traditional methods do not employ sublimated Si and C containing species from a SiC wafer as the source material. The growth in smicrowave heating sublimation sandwich method is performed for time durations of 15 s to 40 s in an atmosphere of UHP-grade nitrogen. Other inert gases such as Ar, He and Xe ionize due to the intense microwave field in the growth chamber. The ΔT between the source wafer and the substrate wafer can be varied from 150 °C to 250 °C by varying the spacing (d) from 300 μm to 600 μm. Growth of SiC nanowires was observed over a very narrow range of both substrate temperature 'T_2' (1650 °C -1750 °C) and ΔT (≈ 150 °C).

A plan-view FESEM image of the nanowires grown at 1700 °C for 40 s is shown in Fig. 13. The nanowires are 10 μm to 30 μm long with diameters in the range of 15 nm to 300 nm. The diameter distribution for the SiC nanowires grown at 1700 °C for 40 s revealed that 42 % of the nanowires have diameters in the range of 15 nm to 100 nm while 14% of nanowires have diameters in excess of 300 nm. EDAX analysis of the nanowires indicated that they mainly

consist of Si and C with traces of nitrogen. The likely sources of this nitrogen are the ambient atmosphere and the nitrogen donor dopant in the source wafer. EDAX spectra taken on the droplets at the nanowire tips consist of the corresponding metal and Si.

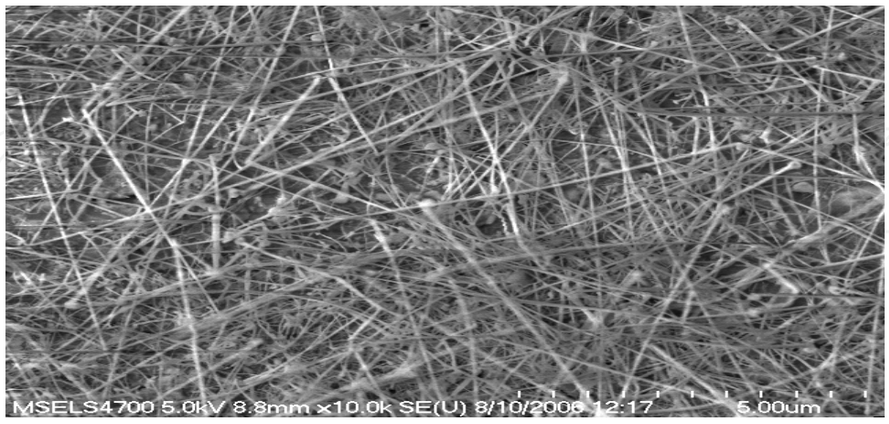

Fig. 13. FESEM image of SiC nanowires grown at T_2 = 1700 °C and ΔT = 150 °C for 40 s.

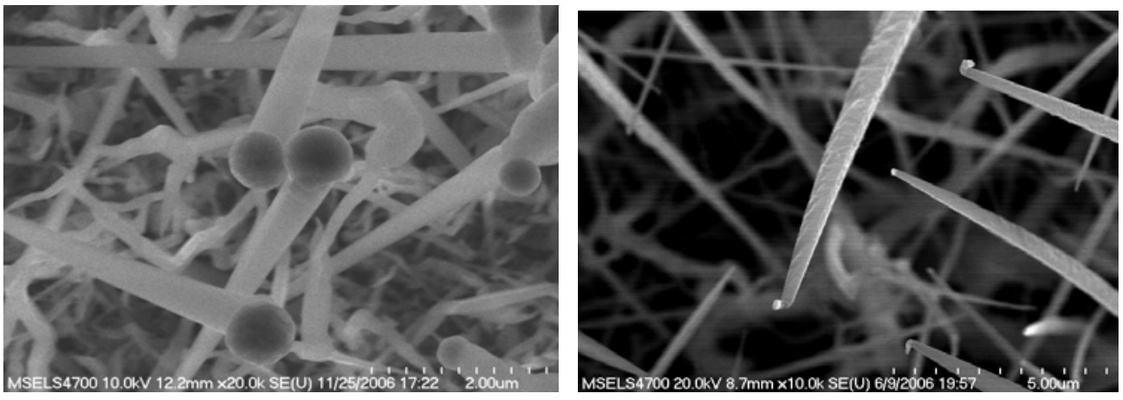

(a) (b)

Fig. 14. (a) Cone-shaped SiC nanostructures grown at T_2 = 1600 °C and ΔT=150 °C; (b) Needle-shaped SiC nanostructures grown at T_2 = 1700 °C and ΔT=250 °C.

In addition to SiC nanowires, growth of cone-shaped and needle-shaped SiC nanostructures was also observed under different growth conditions. For ΔT=150 °C, the substrate wafer temperature in the range of 1550 °C to 1650 °C (for 15 s to 1 min heating cycle duration) yielded mainly cone-shaped quasi 1-D SiC nanostructures (Fig. 14(a)) which are 2 μm – 5 μm long, whereas substrate wafer temperature > 1750 °C (for the same heating cycle durations) resulted in micron-sized SiC deposits (not shown). The "nanocones" shown in Fig. 14(a) taper off along their axis from thick catalytic metal tips. This suggests that the diameter of the droplets increased during the growth of the cones. The diameter of their thin ends are about 10 nm to 30 nm, while the diameter of the broad portion at the top (just under the catalytic metal tips), ranges from 100 nm to 200 nm. The fact that the diameter of the cones increases with growth duration must mean that there is an Oswald ripening effect, i.e. the metal is transferred from the smaller diameter droplets to the larger diameter ones, possibly via surface diffusion (Hannon et al., 2006). The short length of the cones results from a

relatively low SiC growth rate for the experimental conditions under which the cones are grown. Thus, the surface diffusion length for the liquid metal to flow from the smaller diameter droplets to the larger diameter droplets is short.

Increasing the ΔT to 250 ^{o}C (by increasing 'd' from 300 μm to 600 μm) at a substrate wafer temperature (T_2) of 1700 ^{o}C resulted in mainly needle-shaped SiC nanostructures (Fig. 14(b)), which are 50 μm – 100 μm in length. These needles are narrow under the catalytic metal tips. It is obvious that the diameter of the metal droplets catalyzing the needle growth decreases with growth duration. Because the source wafer temperature for needle growth (1900 ^{o}C – 2000 ^{o}C) is high, it is possible that the metal droplets evaporate during crystal growth due to high temperatures in the vicinity of the droplets. The much longer needles (in comparison with the cones) also results in a greater surface diffusion length for the liquid metal to flow between droplets, which might have inhibited significant surface diffusion of the metal.

A much higher density of nanowires in comparison with other 2-D deposits are observed for the growth performed using Fe, Ni, and Pd catalysts. Selected area electron diffraction patterns (not shown) recorded from 10 nanowires were all consistent with a cubic 3C-SiC structure. The growth direction of the nanowire was identified as <112> which is in contrast to the <111> growth direction commonly observed for 3C-SiC nanowires. One of the reasons as to why the <112> growth direction is preferred for the SiC nanowires grown by microwave heating method over the commonly reported <111> direction could be the very high temperatures (1650 ^{o}C – 1750 ^{o}C) used for microwave heating method nanowire growth. The nanowire growth generally occurs along the direction, whose corresponding face has the highest surface energy, so that that particular face is not exposed. The {111} being a three cluster face must have a higher surface energy for SiC at lower temperatures, thereby driving the nanowire growth along the <111> direction. At higher temperatures, the nucleation rate along directions normal to lower atomic density planes such as {110} and {112} is known to be faster than {111}.

Factors affecting the SiC crystal polytype are the temperature (Knippenberg, 1963) and the pressure in the growth chamber, the polarity of the seed crystal, the presence of certain impurities and the Si/C ratio. Under more Si-rich (C-rich) conditions the formation of the cubic (hexagonal) polytype should be preferred (Omuri et al., 1989). Nucleation far from equilibrium conditions and a nitrogen atmosphere has been generally assumed to stabilize the cubic polytype (Limpijumnong and Lambrecht, 1998). This is supported by nucleation theory. Furthermore, 3C-SiC has the lowest surface energy among all polytypes. Since, in the microwave heating sublimation sandwich method, Si-rich precursor species are present (Si, Si_2C), and nucleation occurs far from equilibrium conditions in a nitrogen atmosphere, the growth of 3C-SiC is to be expected from the above considerations. Furthermore, since nanowires have a large surface to volume ratio, the low surface energy of the 3C-SiC polytype makes it much more favorable to grow 3C-SiC over other polytypes. However, it is worth trying to see if under C-rich precursor and Al vapor pressure conditions the hexagonal polytype SiC nanowires can be grown or not. Controlled diameter SiC nanowire growth is expected by pre-patterning the catalyst metal layer to desired dimensions, which controls the diameter of the catalyst liquid droplet during growth.

12. Other applications of microwave heating

Though microwave heating so far has been mainly used for activating ion-implanted and in-situ doped dopants in SiC and GaN, and for growing SiC nanowires, it can be used for other

high-temperature device processing steps such as ohmic contact alloying. Since, the thickness of metal layers used for contacts in semiconductor device fabrication are in the same order as the skin depth, microwave heating is suitable for contact alloying and for formation of silicide films on substrates. Annealing temperature and temperature ramp rates have a profound effect on contact surface morphology and contact resistance, which are two important figures of merit of the ohmic contacts. Hence, microwave heating is desirable for forming ohmic contacts. Because ohmic contacts are always formed on heavily doped regions, differential heating of these regions helps in obtaining high-performance ohmic contacts without heating other regions of the devices.

Microwave heating is also attractive for achieving very high temperatures required for the activation of ion-implantation and in-situ doped impurities in other large bandgap materials such as diamond.

After processing, the semiconductor devices need to be bonded to the carrier and then hermetically sealed. Rapid and selective heating properties of microwaves are very useful for bonding and hermetic sealing of discrete semiconductor devices, and micro-electro-mechanical-system (MEMS) and integrated circuit (IC) devices to the carrier substrate. In some applications the bonding material used should be strong, chemically resistive and withstand high temperatures. Traditional Pb-Sn alloys are not good for these applications. Noble metals such as Au, Cr, Ni and Pt; glass; and ceramics are very good candidates as the bonding materials for these applications, but require high bonding temperatures due to their high melting point. Microwave heating is very attractive in reaching these high temperatures rapidly in the targeted area to be heated without adversely affecting the integrity of MEMS or IC devices to be bonded (Y. Tian and M.Y. Tian, 2009).

Microwave heating is also attractive to form stochiometric composition thin films of compounds such as $In_{2-x}Fe_xO_3$ on any substrate material. Since SiC is an excellent absorber of microwaves, it can be used as a susceptor to evaporate the compound. The compound in powder form can be placed on the SiC susceptor, which is coupled to the microwaves coming from a microwave head. As soon as the microwave power source is turned on, the compound is heated to a temperature greater than the evaporation temperature of all the constituent elements of the compound. This feature leads to the formation of the intended compound film on a nearby substrate, whose composition is similar to that of the powdered compound source material.

Microwave heating can be made as a part of multi-chamber semiconductor epitaxial growth systems for performing ultra-fast in-situ annealing of epitaxial layers in the intermittent stages of the growth process, without breaking the vacuum. Ultra-fast intermittent heat treatment helps to decrease dislocation density in epitaxial layers grown on lattice mismatched substrates (Chen et al., 2008).

13. Acknowledgment

Author thanks Dr. Y-L. Tian of LT Technologies for his collaboration with the author on microwave heating. He acknowledges the valuable contributions made by his past and current graduate students: Siddarth Sundaresan, Nadeemullah Mahadik, Madhu Gowda, Geetha Aluri and Anindya Nath, on this work. He also acknowledges the contributions made by Dr. Syed Qadri of the Naval Research Laboratory; Dr. Roberta Nipoti of IMM-CNR, Bologna, Italy; and Dr. Albert Davydov of NIST. He further acknowledges the financial support provided by the National Science Foundation, the Army Research Office

(ARO) and the DARPA (through the U.S. Naval Research Laboratory contract # N0017310-2-C006).

14. References

Aluri, G.S., Gowda, M., Mahadik, N.A., Sundaresan, S.G., Rao, M.V., Schreifels, J.A., Freitas, Jr., J.A., Qadri, S.B., and Tian, Y-L. (2010). Microwave annealing of Mg-implanted and *in situ* Be-doped GaN. *Journal of Applied Physics*, Vol. 108, 083103

Amada, H. (1987). Method and Apparatus for Microwave Heat-treatment of a Semiconductor Wafer, US Patent No. 4,667,076, May 19

Andrievski, R.A. 2009. Synthesis, Structure and Properties of Nanisized Silicon Carbide. *Review of Advanced Material Science*, Vol. 22, pp. 1-20

Capano, M.A., Ryu, S., Melloch, M.R., Cooper, Jr., J.A., and Buss, M.R. (1998). Dopant activation and surface morphology of ion implanted 4H- and 6H-silicon carbide. *Journal of Electronic Materials,* Vol. 27, No. 7, pp. 370-376

Chen, Y., Farrell, S., Brill, G., Wijewarnasuriya, P., and Dhar, N. (2008). Dislocation reduction in CdTe/Si by molecular beam epitaxy through in-situ annealing. *Journal of Crystal Growth*, Vol. 310, pp. 5303-5307

Fang, X., Hu, L., Ye, C., and Zhang, L. 2010. One-dimensional inorganic semiconductor nanostructures: A new carrier for nanosensors. *Pure and Applied Chemistry*, Vol. 82, No. 11, pp. 2185-2198

Fan, J.Y., Wu, X.L., Chu, P.K. 2006. Low-dimensional SiC nanostructures: Fabrication, luminescence, and electrical properties. *Progress in Material Science*, Vol. 51, No. 8, November, pp. 983-1031

Feng, Z.C. (ed.) 2006). *III-Nitride Semiconductor Materials*, Imperial College Press, London

Fukano, T., Ito, T., and Ishikawa, H. (1985). Microwave Annealing for Low Temperature VLSI Processing. *IEDM Technical Digest*, Vol. 31, pp.224-227

Gardner, J.A., Rao, M.V., Tian, Y.L., Holland, O.W., Roth, E.G., Chi, P.H., Ahmad, I. (1997). Rapid Thermal annealing of ion implanted 6H-SiC by microwave processing. *Journal of Electronic Materials*, Vol. 26, No. 3, pp. 144-150

Ghandhi, S.K. (1994). *VLSI Fabrication Principles: Silicon and Gallium Arsenide* (2nd edition), Wiley-Interscience, ISBN:0471580058, New York

Handy, E.M., Rao, M.V., Holland, O.W., Chi, P.H., Jones, K.A., Derenge, M.A., Vispute, R.D., and Venkatesan, T. (2000). Al, B, and Ga, ion-implantation doping of SiC.*Journal of Electronic Materials*, Vol. 29, pp. 1340-1345.

Hannon, J.B., Kodambaka, S., Ross, F.M., and Tromp, R.M. (2006). The influence of the surface migration of gold on the growth of silicon nanowires. *Nat ure*, Vol. 440, March, pp. 69-71

Heera, V., Mucklich, A., Dubois, C., Voelskow, M., and Skorupa, W. (2004). Layer morphology and Al implant profiles after annealing of supersaturated, single-crystalline, amorphous, and nanocrystalline SiC. *Journal of Applied Physics*, Vol. 96, No. 5, pp. 2841-2852

Huang, Y., Lieber, C.M. 2004. Integrated nanoscale electronics and optoelectronics : Exploring nanoscale science and technology through semiconductor nanowires. *Pure and Applied Chemistry*, Vol. 76, No. 12, pp. 2051-2068

Jenny, J. R., Malta, P., Tsvetkov, V.F., Das, M.K., Hobgood, McD, Carter, C.H., Kumar, R.J., Borrego, J.M., Gutman, R.J., Aavikko, R. (2006). Effects of annealing on carrier lifetime in 4H-SiC. *Journal of Applied Physics*, Vol. 100, No. 11, 113710

Kato, T., Kinoshita, A., Wada, K., Nishi, T., Hozomi, E., Taniguchi, H., Fukuda, K. and Okumura, H. (2010). Morphology improvement of step bunching on 4H-SiC wafers by polishing technique. *Material Science Forum*, Vol. 645-648, April, pp. 763-765

Knippenberg, W.F. (1963). Growth phenomenon in silicon carbide. *Phillips Research Reports*, Vol. 18, No. 3, pp. 161-274

Law, M., Goldberger, J., Yang, P. (2004). "Semiconductor nanowires and nanotubes. *Annual Review of Materials Research*, Vol. 34, August, pp. 83-122

Limpijumnong, S., and Lambrecht, W.R.L. (1998). Total energy differences of SiC polytypes revisited. *Physics Review* B, Vol. 57, pp. 12017-12022

Mahadik, N.A.Qadri, S.B., Sundaresan, S.G., Rao, M.V., Tian. Y., and Zhang, Q. (2009). Effects of microwave annealing on crystalline quality of ion-implanted SiC epitaxial layers. *Surface and Coatings Technology*, Vol. 203, pp. 2625-2627

Negoro, Y., Katsumoto, K., Kimoyo, T., and Matsunami, H. (2004). Electronic Behaviors of High-Dose Phosphorus-Ion Implanted 4H-SiC (0001). *Journal of Applied Physics*, Vol. 96, No. 1, July, pp. 224-228

Omuri, M., Takei, H., and Hukuda, T. (1989). *Japanese Journal of Applied Physics*, Vol. 28, pp. 1217-

Ottaviani, L., Blondo, S., Morata, S., Palais, O., Sauvage, T., and Torregrosa, F. (2010). Influence of Heating and Cooling Rates of Post-implantation Annealing Process on Al-implanted 4H-SiC Epitaxial Samples. *Materials Science Forum*, Vols. 645-648, pp. 717-720

Pearton, S.J., Abernathy, C.R., Ren, F. (2006). *Gallium Nitride Processing for Electronics,Sensors, and Spintronics*, Springer-Verlag, ISBN:1-85233-935-7, London

Phelps, G.J., Wright, N.G., Chester, E.G., Johnson, C.M., and O'Neill, A.G. (2002). Step bunching fabrication constraints in silicon carbide. *Semiconductor Science & Technology*, Vol. 17, No. 5, May, pp. L17-L21.

Poggi, A., Bergamini, F., Nipoti, R., Solmi, Canino, M., S., Carnera, A. (2006). Effects of heating ramp rates on the characteristics of Al implanted 4H-SiC junctions. *Applied Physics L etters*, Vol. 88, No. 16, April,162106.

Rambach, M., Schmid, F., Krieger, M., Frey, L., Bauer, A.J., Pensl, G., and Ryssel, H. (2005). Implantation and annealing of aluminum in 4H silicon carbide. *Nuclear Instruments and Methods in Physics Research* B, Vol. 237, No. 1-2, August, pp. 68-71

Rambach, M., Bauer, A.J., , and Ryssel, H. (2008). Electrical and topographical characterization of aluminum implanted layers in 4H silicon carbide. *Physica Status Solidi* (b),Vol. 245, No. 7, July, pp.1315-1326

Rao, M.V., Tucker, J.B., Ridgway, M.C., Holland, O.W., Capano, M.A., Papanicolaou, N., and Mittereder, J. (1999). Ion-implantation in bulk semi-insulating 4H-SiC. *Journal of Applied Physics*, Vol. 86, No. 2, pp. 752-758.

Rao, M.V., Nath, A., Nipoti, R., Qadri, S.B., and Tian, Y-L. (2010). Annealing of ion-implanted 4H-SiC, *AIP Proceedings : 18th International conference on Ion-implantation Technology (IIT 2010)*, kyoto, Japan, June 6-11, 2010.

Russell, S.D., and Ramirez, A.D. (1999). In situ boron incorporation and activation in silicon carbide using excimer laserrecrystallization. *Applied Physics Letters*, Vol. 74, No. 22, May, pp. 3368-3370

Saddow, S.E., Agarwal, A.K., (eds. (2004) *Advances in Silicon Carbide Processing and Applications*, Artech House, ISBN:1-58053-740-5, Norwood, MA, USA.

Seshadri, S., Eldridge, G.W., Agarwal, A.K. (1998). Comparison of the annealing behavior ofhigh-dose nitrogen-, aluminum-, and boron-implanted 4H–SiC. *Applied Physics Letters*, Vol. 72, No. 16, pp. 2026-2028.

Scovell, P.D. (1984). Method of Reactivating Implanted Dopants and Oxidation of Semiconductor Wafers by Microwaves, U.S. Patent No. 4,490,183, Dec. 25

Spinter, M.R., Palys, R.F., and Beguwala, M.M. (1981). *Low Temperature Microwave Annealing of Semiconductor Devices*, U.S. Patent No. 4,303,455, Dec. 1

Storasta, L. and Tsuchida, H. (2007). Reduction of traps and improvement of carrier lifetimein 4H-SiC epilayers by ion implantation. *Applied Physics Letters*, Vol. 90, No. 6, 062116

Sundaresan, S.G., Rao, M.V., Tian, Y., Schreifels, J.A., Wood, M.C., Jones, K.A., Davydov, A.V. (2007). Comparison of solid-state microwave annealing with conventional furnace annealing of ion-implanted SiC. *Journal of Electronic Materials*, Vol. 36, No. 4, pp. 324-331

Sundaresan, S.G., Rao, M.V., T-L. Tian, Ridgway, M.C., Schreifels, J.A., Kopanski, J.J. (2007). Ultrahigh-temperature microwave annealing of Al^+- and P^+-implanted 4H-SiC. *Journal of Applied Physics*, Vol. 101, 073708

Sundaresan, S.G., Davydov, A.V., Vaudin, M.D., Levin, I., Maslar, J.E., Tian, Y-L., and Rao, M.V. (2007). Growth of silicon carbide nanowires by a microwave heating-assisted physical vapor transport process using Group VIII metal catalysts. *Chemistry of Materials*, Vol. 19, pp. 5531-5537

Sundaresan, S.G., Murthy, M., Rao, M.V., Schreifels, J.A., Mastro, M.A., Eddy, Jr., C.R., Holm, R.T., Henry, R.L., Freitas, Jr., J.A., Gomar-Nidal, E., Vispute, R.D., and Tian, Y-L. (2007). Characteristics of in-situ Mg-doped GaN epi-layers subjected to ultra-high-temperature microwave annealing using protective caps. *Semiconductor Science and Technology*, Vol. 22, pp. 1151-1156

Sundaresan, S.G., Mahadik, N.A., Qadri, S.B., Schreifels, J.A., Tian, Y-L., Zhang, Q., Gomar-Nadal, E., Rao, M.V. (2008). Ultra-low resistivity Al^+ implanted 4H-SiC obtained by microwave annealing and a protective graphite cap. *Solid-State Electronics*, Vol. 52, pp. 140-145

Tanaka, Y., Tanoue, H., Arai, K. (2003). Electrical activation of the ion implanted phosphorus in 4H-SiC by excimer laser annealing, *Journal of Applied Physics*, Vol. 93, pp. 5934-5936

Tian, Y., & Tian, M.Y. (2009). Method and Apparatus for Rapid Thermal Processing and Bonding of Materials Using RF and Microwaves. U.S. Patent No. US 7,569,800, Aug. 4

Tian, Y-L. (2009). Microwave based technique for ultra-fast and ultra-high temperature thermal processing of compound semiconductors and nano-scale Si semiconductors, *Proccedings of 17th IEEE International Conference on Advanced Thermal Processing of Semiconductors – RTP* 2009

Thompson, D.C., Decker, J., Alford, T.L., Mayer, J.W., Theodore, N.D. (2007). Microwave Activation of Dopants & Solid Phase Epitaxy in silicon, *MRS Proceedings*, Vol. 989, Title: Amorphous and Polycrystalline Thin-Film Silicon Science and Technology—2007, Spring 2007 Meeting, Symposium A

Vassilevski, K.V., Wright, N.G., Nikitina, I.P., Horshall, A.B., O'Neill, A.G., Uren, M.J., Hilton, K.P., Masterton, A.G., Hydes, A.J., and Johnson, C.M. (2005). Protection of selectively implanted and patterned silicon carbide surfaces with graphite capping layer during post-implantation annealing. *Semiconductor Science and Technology*, Vol. 20, pp. 271-278

Vathulya, V.R., and White, M.H. (2000). Characterization and performance comparison of the power DIMOS structure fabricated with a reduced thermal budget in 4H and 6H-SiC. *Solid-State Electronics*, Vol. 44, pp. 309-315.

Zhang, S.I., Buchta, R., and Sigurd, D. (1994). Rapid thermal processing with microwave heating. *Thin Solid Films*, Vol. 246,No. 1-2, 15 June, pp. 151-157

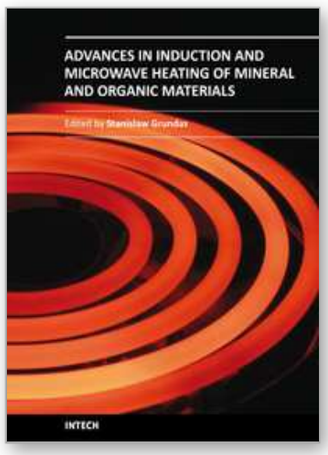

Advances in Induction and Microwave Heating of Mineral and Organic Materials

Edited by Prof. StanisÅ‚aw Grundas

ISBN 978-953-307-522-8
Hard cover, 752 pages
Publisher InTech
Published online 14, February, 2011
Published in print edition February, 2011

The book offers comprehensive coverage of the broad range of scientific knowledge in the fields of advances in induction and microwave heating of mineral and organic materials. Beginning with industry application in many areas of practical application to mineral materials and ending with raw materials of agriculture origin the authors, specialists in different scientific area, present their results in the two sections: Section 1-Induction and Microwave Heating of Mineral Materials, and Section 2-Microwave Heating of Organic Materials.

How to reference

In order to correctly reference this scholarly work, feel free to copy and paste the following:

Mulpuri V. Rao (2011). Ultra-Fast Microwave Heating for Large Bandgap Semiconductor Processing, Advances in Induction and Microwave Heating of Mineral and Organic Materials, Prof. StanisÅ‚aw Grundas (Ed.), ISBN: 978-953-307-522-8, InTech, Available from: http://www.intechopen.com/books/advances-in-induction-and-microwave-heating-of-mineral-and-organic-materials/ultra-fast-microwave-heating-for-large-bandgap-semiconductor-processing

INTECH
open science | open minds

InTech Europe
University Campus STeP Ri
Slavka Krautzeka 83/A
51000 Rijeka, Croatia
Phone: +385 (51) 770 447
Fax: +385 (51) 686 166
www.intechopen.com

InTech China
Unit 405, Office Block, Hotel Equatorial Shanghai
No.65, Yan An Road (West), Shanghai, 200040, China
中国上海市延安西路65号上海国际贵都大饭店办公楼405单元
Phone: +86-21-62489820
Fax: +86-21-62489821

IntechOpen